

Research Article

1H-MRS Observation of Frontal White Matter Metabolites in Human Natural Aging and Early Cognitive Decline in Vivo

Qi Xie^{1,*}, † , Zhi-lin Tan^{1,2}, † , Ya-jie Wang^{1,3} , Hui-xian Chen¹¹Medical Imaging Department of Nansha, Guangzhou First People's Hospital, School of Medicine, South China University of Technology, Guangzhou, China²Department of Radiology, Shunde Hospital, Southern Medical University (The First People's Hospital of Shunde), Shunde, China³Department of Radiology, West China Hospital, Sichuan University, Chengdu, China

Abstract

Proton magnetic resonance spectroscopy (1H-MRS) enables noninvasive in vivo detection of biochemical and neurotransmitter alterations in brain neurons, offering potential for early diagnosis of Alzheimer's disease (AD). This study investigates metabolite distribution patterns in bilateral frontal white matter and imaging biomarkers of early cognitive function across preclinical and prodromal stages of the AD continuum. A cohort of 362 right-handed participants underwent comprehensive neuropsychological assessments. Single-voxel 1H-MRS was employed to acquire metabolite spectra from bilateral frontal white matter, complemented by venous blood analysis for AD-associated genes and toxic proteins. Statistical analysis revealed the following key findings. Normal Controls (NC): (1) Higher relative concentrations of N-acetyl-aspartate/N-acetyl aspartyl-glutamate (NAA+NAAG) and glycerol-phosphocholine/phosphocholine (GPC+PCho) were observed in left versus right frontal white matter. (2) Age-related decline: NAA+NAAG levels in left frontal white matter demonstrated progressive reduction from younger to older age groups. (3) The elderly group exhibited significantly lower glutamate/glutamine (Glu+Gln) concentrations in left frontal white matter compared to middle-aged and younger groups. Mild Cognitive Impairment (MCI): (1) Inverse correlation between Auditory Verbal Learning Test (AVLT) scores and right frontal NAA+NAAG content. (2) Positive associations between Shape Trail Test (STT-A/B) completion times and right frontal myo-inositol (mIns) levels. Left frontal Glu+Gln concentrations correlated positively with plasma biomarkers: amyloid β -protein (A β 1-42), total tau (t-tau), and phosphorylated tau181 (p-tau181). These 1H-MRS-detected metabolite alterations in bilateral frontal white matter may reflect both physiological brain aging and AD-related pathological changes, suggesting their utility as potential diagnostic indicators for early-stage AD. The integration of metabolic profiling with established biomarkers could enhance predictive accuracy in the AD continuum.

Keywords

Natural Aging, Subjective Cognitive Decline, Mild Cognitive Impairment, Proton Magnetic Resonance Spectroscopy, Neuro-metabolites, In Vivo

*Correspondence: Qi Xie (xieqi8@yeah.net), Qi Xie (eyqixie@scut.edu.cn)

† Qi Xie and Zhi-lin Tan are co-first authors.

Received: 11 April 2026; Accepted: 26 April 2026; Published: 11 May 2026



1. Introduction

Amidst the global demographic shift toward an aging population, Alzheimer's disease (AD)—characterized primarily by progressive cognitive impairment—has emerged as a critical public health concern [1]. The pathogenesis of AD follows a protracted temporal trajectory, clinically manifesting as a continuum: initiating with subjective cognitive decline (SCD) in the preclinical phase, advancing to mild cognitive impairment (MCI) during the prodromal stage, and ultimately culminating in dementia-related cognitive dysfunction. This multi-stage progression typically spans years to decades [1].

Since cognitive function remains intact in individuals with SCD, this population represents the optimal candidates for early interventions aimed at delaying or even preventing cognitive deterioration [2]. In contrast, patients with MCI exhibit heterogeneous clinical trajectories, including stabilization of cognitive status, reversion to normal cognition, or progression to AD [3]. Consequently, the early identification of SCD and MCI patients at risk of cognitive decline is of paramount importance [1-3].

Magnetic resonance spectroscopy (MRS) stands as the sole noninvasive imaging modality capable of detecting *in vivo* biochemical and neurotransmitter alterations within brain neurons, devoid of radiation exposure [3-5]. The majority of proton MRS (1H-MRS) investigations in AD and MCI cohorts have predominantly targeted the temporal lobe, hippocampus, para-hippocampal gyrus, amygdala, and posterior cingulate gyrus as regions of interest. Emerging evidence indicates that a decline in N-acetylaspartate (NAA) levels is a widespread phenomenon across multiple brain regions in AD and MCI patients, frequently concomitant with elevated myo-inositol (mIns) and a marked reduction in glutamate (Glu). These metabolic perturbations exhibit a significant correlation with the severity of cognitive deficits [4-6].

The pathological hallmarks of AD encompass extracellular amyloid β -protein ($A\beta$) plaques and intracellular neurofibrillary tangles composed of hyperphosphorylated tau protein, culminating in progressive neurodegeneration, synaptic loss, cognitive dysfunction, and ultimately dementia [1]. These brain pathophysiological alterations typically manifest 10 to 15 years prior to clinical symptom onset [1, 3-5]. $A\beta$ -positron emission tomography (PET) studies have delineated a distinct spatiotemporal pattern of $A\beta$ deposition, with the frontal lobe identified as one of the earliest brain regions affected [4, 7, 8].

Accounting for approximately one-third of the human brain's volume, the frontal lobe harbors extensive neural networks interconnected with multiple brain regions, playing a pivotal role in memory formation and abstract reasoning. Pathological changes in the frontal lobe are thus closely associated with cognitive dysfunction [9]. We hypothesize that neuroimaging evidence of metabolic abnormalities in the frontal lobe may emerge earlier during the trajectory of cognitive decline.

Current literature remains limited regarding the correlation between cognitive status and frontal lobe metabolites assessed via 1H-MRS. Emerging evidence indicates elevated glutamate complex (GLX) levels and increased to total creatine ratios (mIns/tCR) in the medial frontal cortex of MCI patients, concomitant with reduced γ -aminobutyric acid (GABA) concentrations [10]. Our prior functional MRI (fMRI) investigations demonstrated significantly higher regional homogeneity (ReHo) values within left hemispheric regions of the frontoparietal network—including the Rolandic operculum, insular-inferior frontal gyrus junction, precentral gyrus, and middle frontal gyrus—in MCI subjects compared to normal controls (NC) [11].

This ReHo elevation potentially represents a neuroplastic adaptation of cortical networks in MCI pathophysiology, serving as a compensatory mechanism against incipient functional deterioration in linguistic processing, memory consolidation, and executive functions [11]. The underlying neurobiological basis warrants further investigation: whether this diffuse frontal ReHo augmentation stems from (1) direct $A\beta$ -induced neuronal toxicity or (2) secondary functional reorganization following structural disconnection of subcortical white matter tracts—critical conduits for cortical neural information transfer—remains to be elucidated.

This study enrolled a community-based cohort of 362 participants, stratified into NC, SCD, SCD-plus (SCD-p), and MCI groups. Utilizing 1H-MRS, we investigated alterations in neuro-metabolites within the bilateral frontal white matter and examined their associations with plasma levels of toxic proteins across cognitive strata. Our findings contribute preliminary insights into potential imaging biomarkers capable of differentiating physiological aging from early-stage neurodegenerative pathologies.

2. Materials and Methods

2.1. Ethics

This prospective cohort study, conducted in a community-based population, received ethical approval from the Ethics Committee of Guangzhou First People's Hospital (Approval No. K-2019-166-01). In accordance with the principles of the Helsinki Declaration (2013 revision), all participants provided written informed consent prior to undergoing study-related medical examinations.

2.2. Participant

The procedures for participant recruitment and research data collection were consistent with those employed in our project team's prior study [12], as illustrated in Figure 1.

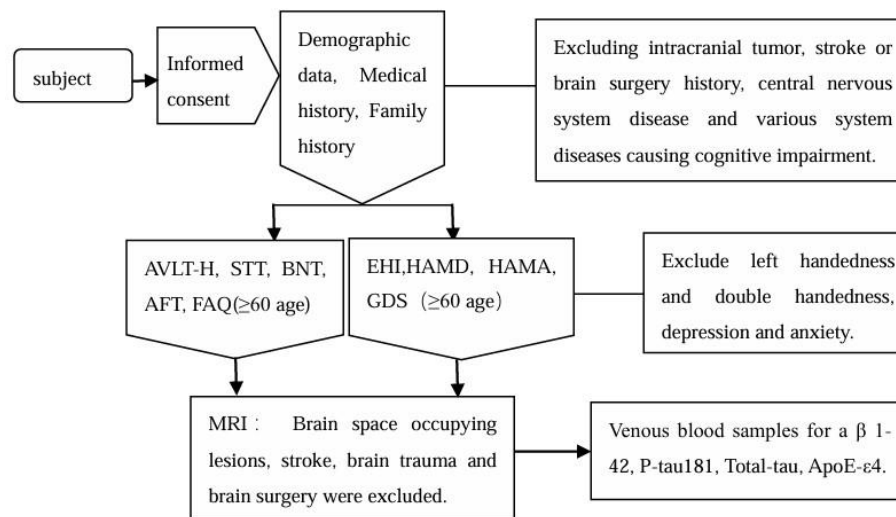


Figure 1. Flow chart of subject recruitment.

All participants underwent comprehensive neuropsychological and cognitive evaluations. Standardized objective assessments included: (1) the Edinburgh Handedness Inventory (EHI) for lateralization screening; (2) the Hamilton Depression Rating Scale (HAMD-17) and Hamilton Anxiety Rating Scale (HAMA) for affective symptom quantification. Cognitive domains were evaluated through: (a) memory (Auditory Verbal Learning Test-Hua Shan version, AVLT-H), (b) executive function (Shape Trail Test, STT), and (c) language proficiency (Boston Naming Test, BNT; Animal Fluency Test, AFT). For geriatric participants (age ≥ 60 years), supplementary instruments were administered: the Geriatric Depression Scale (GDS-15) and Functional Activities Questionnaire (FAQ) to detect prodromal or mild neurocognitive disorders.

Inclusion Criteria: (1) Aged 18-79 years with random gender distribution; (2) Minimum 7 years of formal education; (3) Ethnic Han Chinese population; (4) Right-handedness confirmed by Edinburgh Handedness Inventory (score $> +40$). **Exclusion Criteria:** (1) Left-handed or ambidextrous individuals (EHI score $\leq +40$); (2) History of intracranial space-occupying lesions, cerebrovascular accidents, or neurosurgical interventions; (3) Central nervous system disorders potentially affecting cognition (e.g., Parkinson's disease, major depressive disorder, generalized anxiety disorder, metabolic encephalopathy); (4) Systemic diseases with known cognitive impact (e.g., severe hepatic/renal impairment, thyroid dysfunction); (5) MRI scans failing to meet quality control standards for analysis; (6) Participants unable to complete neuropsychological assessments or withdrawing from study participation.

The final cohort comprised 362 eligible participants (178 males, 49.2%; 184 females, 50.8%) with a mean age of 46.73 ± 13.93 years (range: 18-79 years) and mean educational attainment of 13.54 ± 3.70 years (range: 7-22 years). Gender-stratified analysis revealed comparable demographic profiles: males exhibited mean age 46.77 ± 12.85 years and education

duration 13.49 ± 3.63 years, while females demonstrated mean age 46.70 ± 14.93 years and education duration 13.58 ± 3.78 years. Among the cohort, 283 participants underwent venipuncture with successful apolipoprotein E- $\epsilon 4$ (ApoE- $\epsilon 4$) genotyping results, while quantitative analysis of blood-based biomarkers - including A β 1-42, total tau protein (t-tau), and phosphorylated tau181 protein (p-tau181) - was obtained for 214 cases.

According to the World Health Organization (WHO) criteria for age groups [13], participants were further categorized into three age subgroups including the youth group (≤ 44 years old), the middle-aged group (45-59 years old) and the older group (≥ 60 years old).

2.3. Neuropsychological Evaluation and Cognitive Evaluation

Participants were comprehensively assessed in a standardized, quiet environment by three board-certified clinicians who underwent rigorous protocol training. The evaluation procedures and diagnostic criteria strictly adhered to the established methodology detailed in prior research [12, 14], ensuring inter-rater reliability.

To minimize the impact of confounding variables and enhance the comparability of neuropsychological assessments across varying cognitive states, the raw scores from six tests spanning three cognitive domains—AVLT long-delay recall and recognition, STT-A and STT-B, and AFT and BNT—were standardized using Z-score transformation. The formula for this transformation is detailed below.

$$Z_n = \frac{x_n - \bar{x}}{s}$$

In the above formula, Z_n is the Z score of the n th subject, X_n is the original score of the test of the n th subject, \bar{X} is the average score of the test in all subjects, and s is the standard

deviation of the score of all subjects in the test. The STT test takes the reciprocal of the completion time as the original score of the test. The average Z score of two tests in the same cognitive domain is the combined Z score of the subject in this cognitive domain.

Participants were stratified into four cognitive groups based on established criteria for NC, SCD, SCD-p and MCI [14].

2.4. MR Data Acquisition

2.4.1. MR Examination

MRI examinations were performed using a 3.0T Skyra scanner equipped with a 32-channel phased array head coil (Siemens Medical, Erlangen, Germany). Participants were positioned supine, instructed to breathe calmly, close their eyes, and maintain head immobility throughout the cranial imaging sequence.

Initial conventional MRI sequences were acquired, including axial T2-weighted imaging (T2WI), axial T2 fluid-attenuated inversion recovery (T2-FLAIR), and sagittal three-dimensional T1-weighted volumetric magnetization-prepared rapid gradient-echo (T1_MPRAGE) sequences. Following

image evaluation by board-certified radiologists to exclude intracranial pathologies such as hemorrhage, infarction, or neoplastic lesions, 1H-MRS was performed in the bilateral frontal white matter using a point-resolved spectroscopy (PRESS) sequence. The specific 1H-MRS scanning protocol and primary acquisition parameters are detailed below.

T1_MPRAGE: TR/TE=2530 ms/2.96 ms, TI=1100 ms, FOV= 256 mm×256 mm, matrix =256 × 256, NEX=1, FA=7°, number of slices=192, slice thickness=1 mm, slice gap=0.5 mm, voxels = 1.0 mm × 1.0 mm × 1.0 mm, and scanning time=4 minutes 30 seconds.

1H-MRS (RESS): TR/TE=1500 ms/35 ms, FA=90°, NEX=256, FOV=10 mm×10 mm ×10 mm, bandwidth=1200 Hz, water suppression bandwidth=50 Hz, and scanning time=6 minutes 32 seconds. Receive or transmit gain adjustment, automatic water suppression and intravoxel shimming (if shimming fails, perform manual shimming). Bilateral frontal white matter was selected as the region of interest, and the axial, sagittal, and coronal planes after MPR were used for 1H-MRS localization via t1_mprage images to avoid interference from surrounding ventricular structures and the frontal cortex (Figure 2).

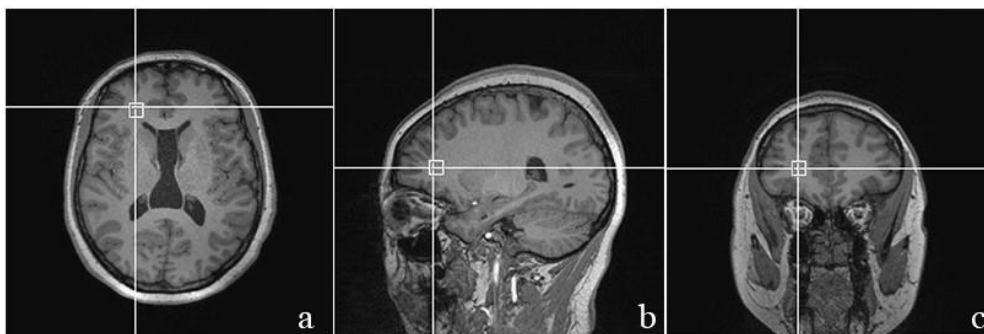


Figure 2. Location map of 1H-MRS (PRESS sequence) for data acquisition of the white matter in the right frontal lobe of the subject. White boxes represent the location of the region of interest (1.0cm × 1.0cm × 1.0cm) in T1_MPRAGE reconstruction axial (a), sagittal (b) and coronal (c) images.

2.4.2. Data Analysis and Quality Control of 1H-MRS

Following completion of 1H-MRS scanning, spectral data in IMA format were exported for analysis. The IMA files were imported into LCModel quantitative spectral analysis software (Stephen Provencher, Version 6.3-1L) with selection of an appropriate basis set (press_te35_3t_v3.basis) - a priori knowledge reference specifically designed by developer Stephen Provencher for the PRESS sequence parameters employed in this study. Automated processing included baseline correction, spectral smoothing, and quantitative analysis. The software generated relative metabolite concentrations and corresponding fitted spectral plots (Figure 3) through its computational algorithms.

The automatically quantified metabolites included: total N-acetylaspartate (tNAA: NAA + N-acetyl aspartylglutamate [NAAG]; chemical shift 2.01-2.04 ppm), the composite peak of total choline-containing compounds (tCho: phosphocholine + glycerophosphocholine [PCho + GPC]; 3.21 ppm), total creatine pool (tCr: creatine + phosphocreatine [Cr + PCr]; 3.03 ppm and 3.96 ppm), myo-inositol (mIns; 3.56 ppm), and the glutamate-glutamine complex (Glx: Glu + Gln; 2.35 ppm and 2.45 ppm). Relative metabolite concentrations were expressed as ratios to the total creatine signal (Cr + PCr), with all quantifications automatically generated by LCModel software. Only metabolite ratios demonstrating a coefficient of variation (CV) <20% in the automated quantification were considered statistically valid for subsequent analysis.

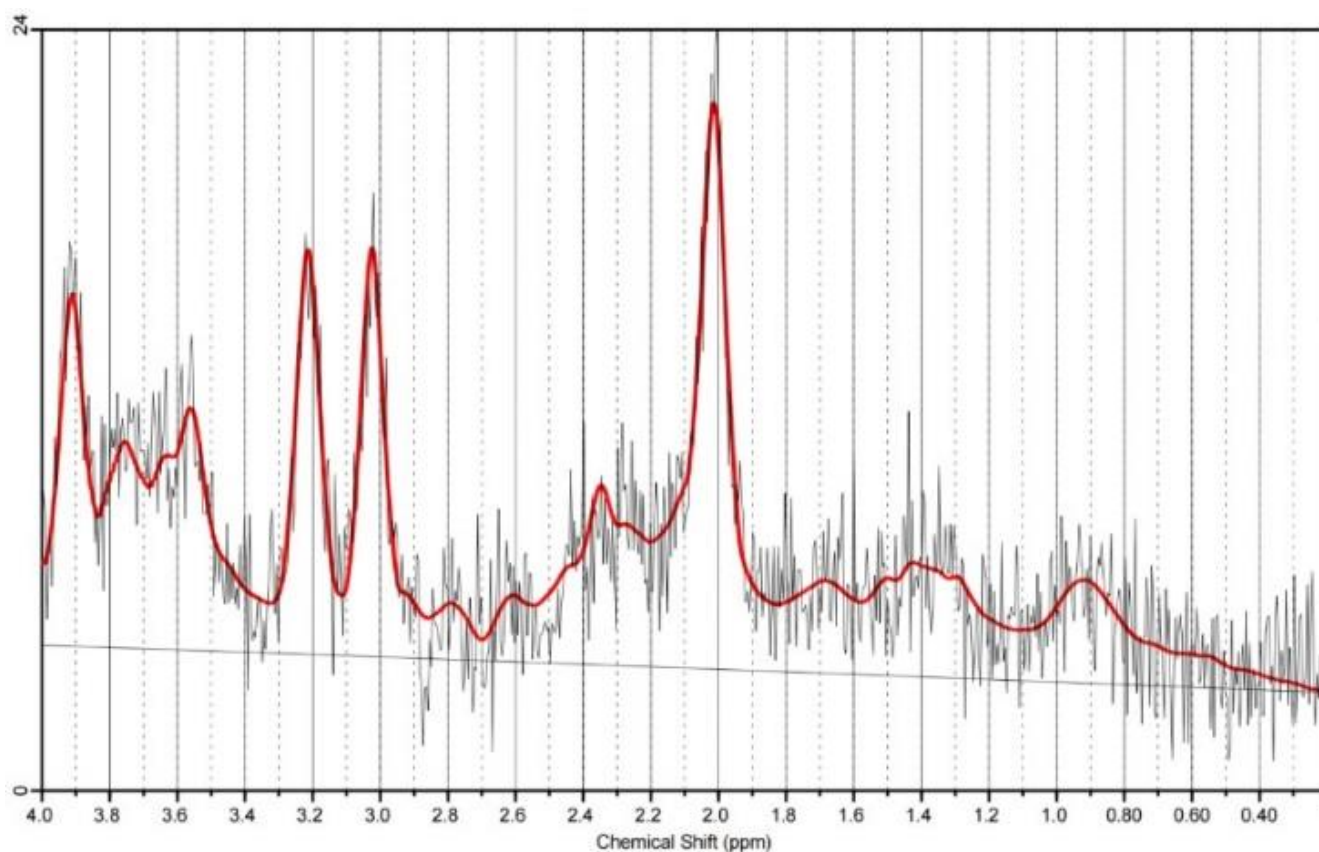


Figure 3. Spectrum of 1H-MRS in right frontal white matter of NC group after LCMoel post-processing.

2.5. Blood Sample Collection and Subsequent Analysis of Relevant Genetic Markers and Pathogenic Protein Levels

Following completion of the aforementioned data collection, participants provided informed consent for venous blood sampling. A trained nurse collected 6 mL of venous blood from either antecubital vein within 24 hours, distributing the sample into three vacuum blood collection tubes. The tubes were gently inverted, stored at 0–4°C, and subsequently transported for laboratory analysis.

Blood sample testing was conducted by Kang Sheng Da Medical Laboratory Co., Ltd. in Wuhan, Hubei Province, utilizing the same methodology as described in our prior study [12, 14].

ApoE-ε4 genotyping was performed using next-generation sequencing (NGS) technology. The target region of ApoE-ε4 was captured in a single step using a customized AD gene multiplex PCR panel (AngsDX™ Custom AD Panel For Illumina, Hangzhou Microgene) on the Illumina NextSeq 550 sequencing platform. The constructed libraries were subsequently sequenced on the NextSeq 550 instrument.

AD-related toxic proteins were quantified using enzyme-linked immunosorbent assay (ELISA). The ELISA kits included human Aβ 1–42 ELISA Kit (Cat# BYS10562B), human total tau protein (t-tau) ELISA Kit (BYS103424B), and

human phosphorylated tau-181 protein (p-tau-181) ELISA Kit (Cat#BYS104511B). All kits were sourced from Shanghai Boyan Biotechnology Co., Ltd., and all procedures were strictly performed according to the manufacturer's instructions. The final concentrations obtained included Aβ1–42 protein (μg/L), t-tau protein (pg/mL), and p-tau-181 protein (ng/L).

2.6. Statistical Analysis

The collected data were compiled into a database using EXCEL 2019 and analyzed with SPSS Statistics (version 25.0; IBM Corp., Armonk, NY, USA). Categorical variables were assessed using χ^2 tests. Normality of continuous variables was evaluated via the Kolmogorov-Smirnov test.

For multi-group comparisons of quantitative data, one-way analysis of variance (ANOVA) was employed for normally distributed variables, while the nonparametric Kruskal-Wallis test (K-W) was used for non-normally distributed data. Post hoc analyses following ANOVA included the Bonferroni correction (assuming homogeneity of variance) or Tamhane's T2 test (for heterogeneous variance). Two-group comparisons were performed using paired-sample t-tests (normal distribution) or the nonparametric Mann-Whitney U test (non-normal distribution).

Aβ1–42, t-tau, and p-tau protein levels (all non-normally

distributed) were compared across cognitive groups via Kruskal-Wallis (K-W) test. Spearman's correlation analyzed associations between blood biomarker levels and 1H-MRS metabolite concentrations.

Statistical significance was set at $p < 0.05$ (95% CI).

3. Results

3.1. Demographic Characteristics Across Cognitive Diagnostic Groups

Table 1 presents the demographic characteristics, neuropsychological assessments, and cognitive scale results of the 362 participants.

Sex distribution did not differ significantly across cognitive groups (χ^2 test, $p = 0.05$). However, marked differences were observed in age, educational attainment, and neuropsychological test scores among the groups (Kruskal-Wallis test, $P < 0.001$). Post-hoc analyses revealed that the MCI group was significantly older than the SCD-p, SCD, and NC groups, while the SCD group was older than the NC group ($P < 0.001$). Similarly, the MCI group had significantly fewer years of education compared to the SCD-p, SCD, and NC groups, and the SCD group had fewer years than the NC group ($P < 0.001$).

The MCI group exhibited significantly poorer performance across all six tests in the three cognitive domains compared to the NC, SCD, and SCD-p groups (Kruskal-Wallis test,

$P < 0.001$). There were no significant differences in memory, executive or language functions among the NC group, SCD group and SCD-p group (Kruskal-Wallis test, $P > 0.05$).

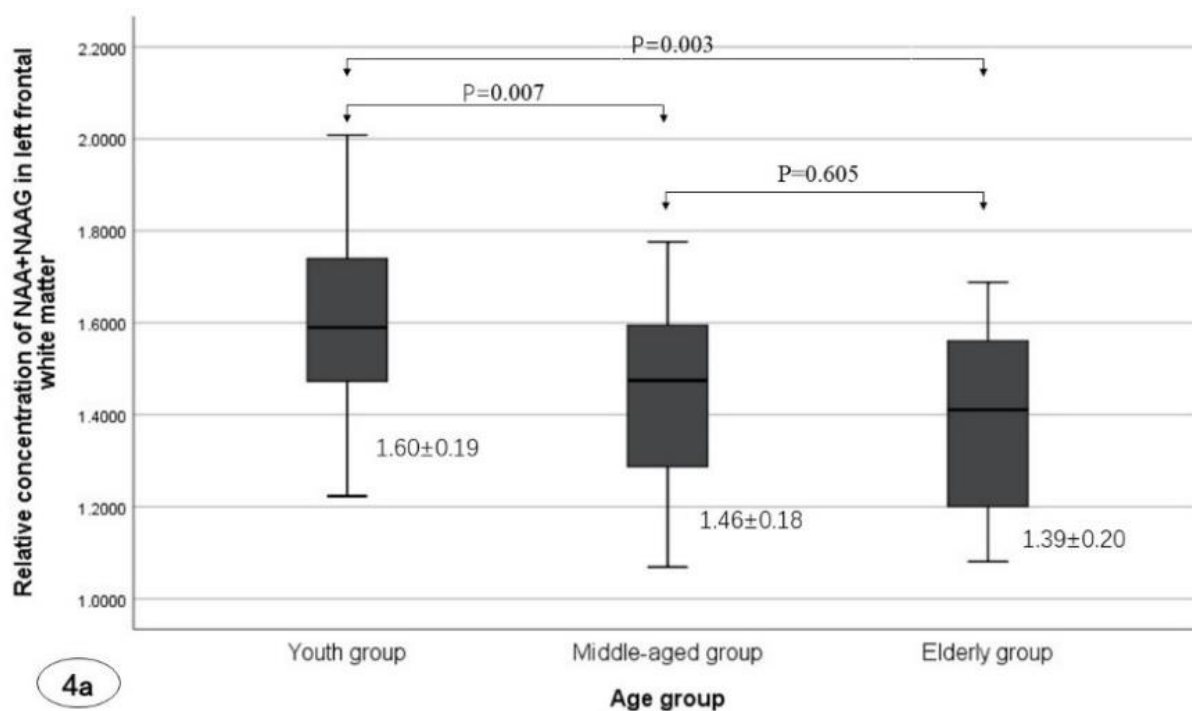
3.2. Metabolite Concentrations in the Bilateral Frontal White Matter of NC Group Participants

3.2.1. Metabolite Concentrations in the Bilateral Frontal White Matter

Table 2 presents the metabolite concentrations in the bilateral frontal white matter of 108 NC participants. Using Cr+PCr as an internal reference, the relative concentrations of NAA+NAAG and GPC+PCh were significantly higher in the left frontal white matter compared to the right (Mann Whitney U test., $P < 0.01$).

3.2.2. Metabolite Concentrations in the Bilateral Frontal White Matter Across Different Age Groups

Table 3 and Figure 4 summarize the demographic characteristics of the different age groups and the comparative analysis of metabolite concentrations in the frontal white matter. A significant, gradual decline in mean years of education was observed across the age groups (Kruskal-Wallis test, $P < 0.001$).



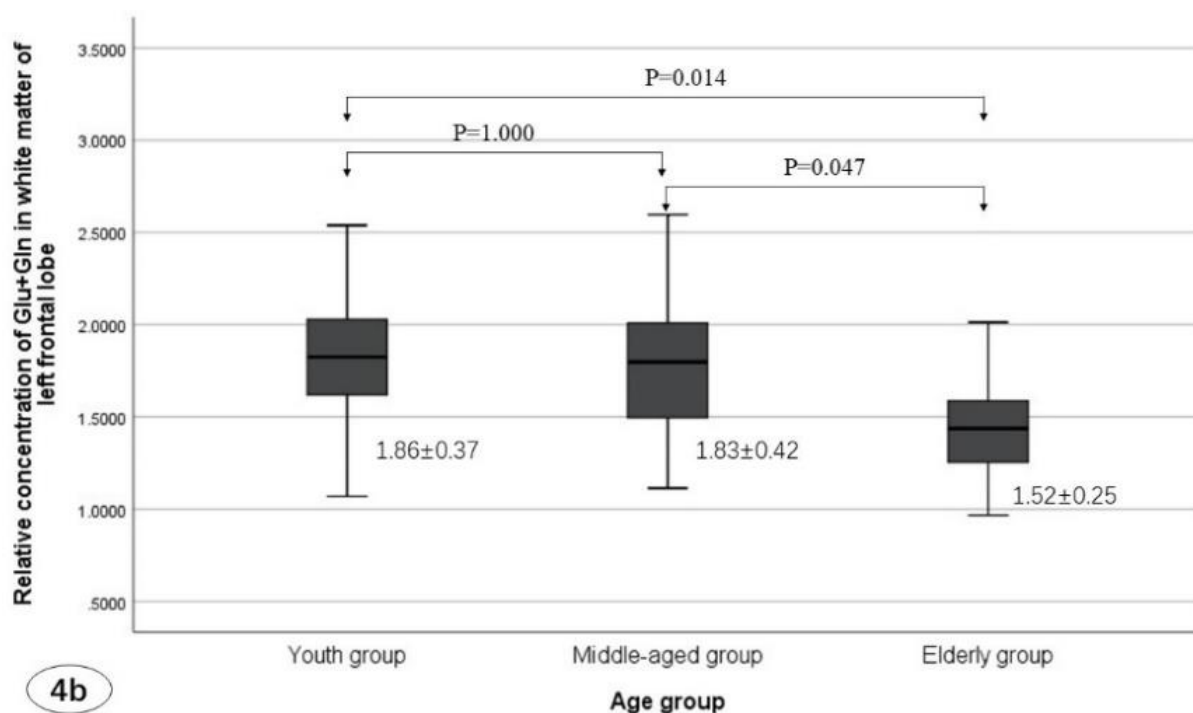


Figure 4. Relative concentrations of NAA+NAAG (a) and Glu+Gln (b) in the left frontal white matter across young, middle-aged, and older adult groups.

Advancing age was associated with a significant decline in the relative concentrations of NAA+NAAG and Glu+Gln in the left frontal white matter (Kruskal-Wallis test, $P < 0.01$). Post-hoc analyses demonstrated significant differences in NAA+NAAG levels among the young, middle-aged, and older adult groups ($P < 0.01$). Additionally, Glu+Gln concentrations in the older group were significantly lower than those in both the young ($P = 0.014$) and middle-aged groups ($P = 0.047$).

3.2.3. Comparative Analysis of Metabolite Concentrations in the Bilateral Frontal White Matter by Sex

In the NC group, male participants (mean age: 42.66 ± 12.68 years) were significantly older than their female counterparts (mean age: 36.54 ± 11.93 years) (Mann-Whitney U test, $P = 0.046$). No significant difference in educational attainment was observed between sexes ($P > 0.05$). After adjusting for age and education as confounding variables, the relative concentrations of NAA+NAAG, GPC+PCh, mIns, and Glu+Gln in the bilateral frontal white matter did not differ sig-

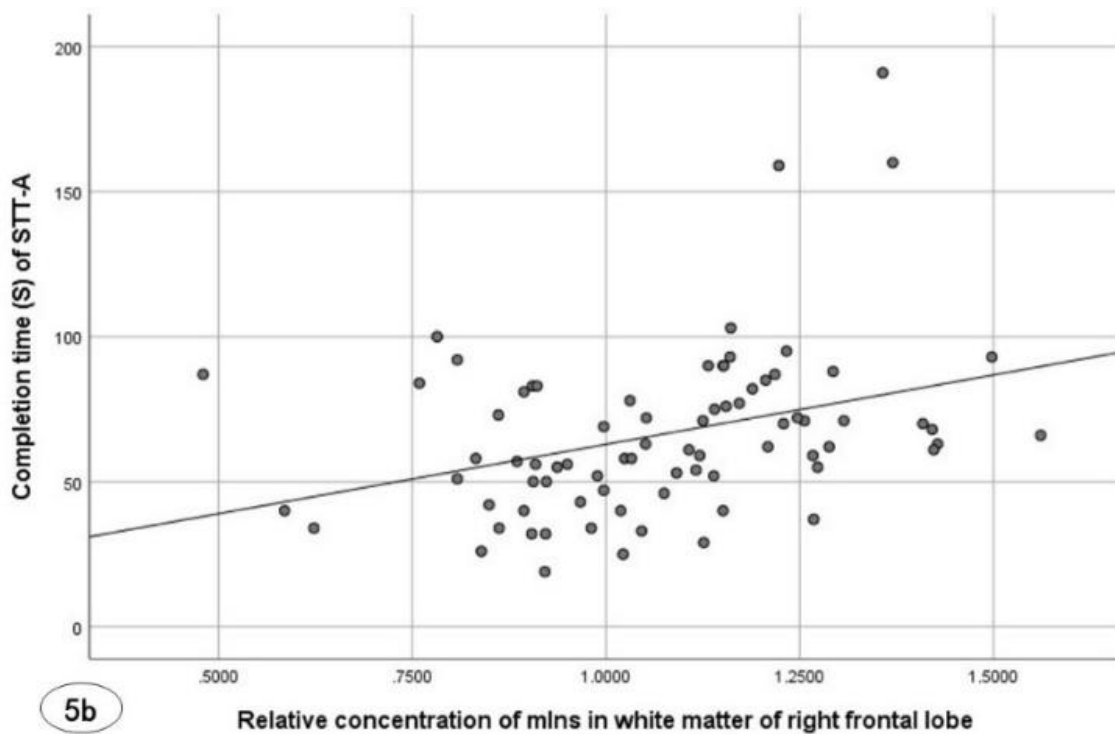
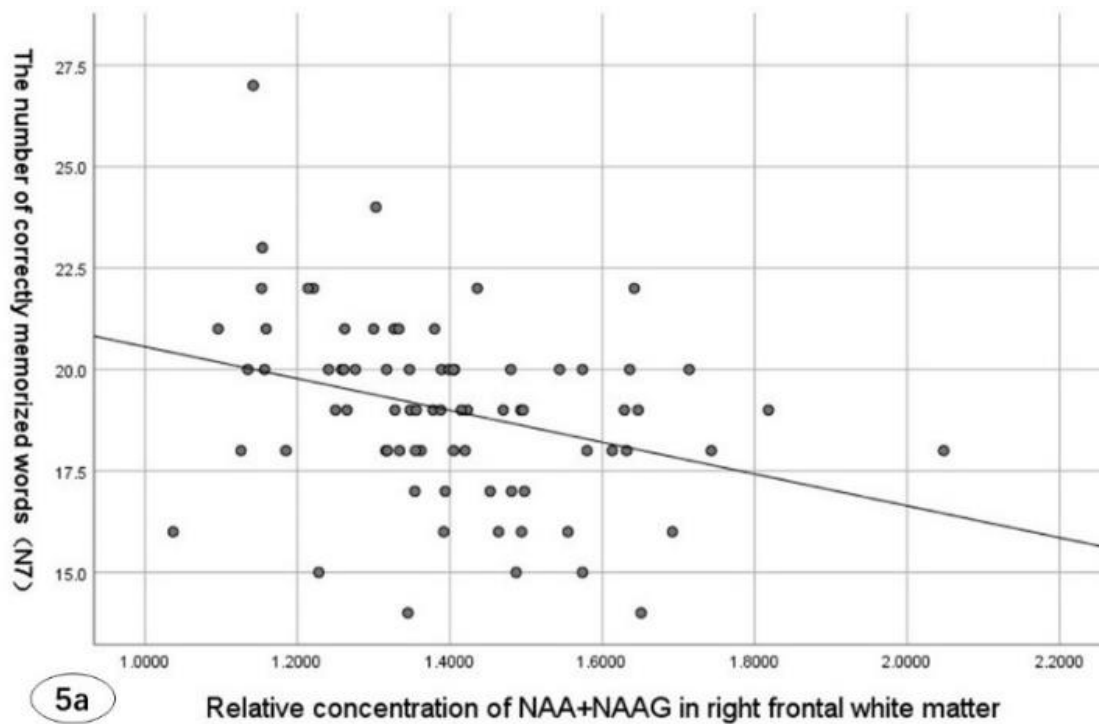
nificantly between males and females ($P > 0.05$). Detailed results are presented in Table 4.

3.3. Comparative Analysis of Metabolite Concentrations in the Bilateral Frontal White Matter Across Cognitive Diagnostic Groups

In the young and middle-aged groups, age demonstrated a significant upward trend (Kruskal-Wallis test, $P < 0.01$), while educational attainment showed a marked decline ($P < 0.01$) from NC to MCI. Among older adults, the proportion of males progressively decreased, with a corresponding increase in females (χ^2 test, $P = 0.011$) across the diagnostic spectrum. Detailed results are presented in Table 5.

ANCOVA was employed to adjust for the confounding effects of age and educational attainment. The analysis revealed no significant differences in metabolite concentrations in the bilateral frontal white matter across cognitive groups (Kruskal-Wallis test, $P > 0.05$). Specific results are detailed in Table 6.

3.4. Association Between Relative Metabolite Concentrations in Bilateral Frontal White Matter and Neuropsychological Test Scores



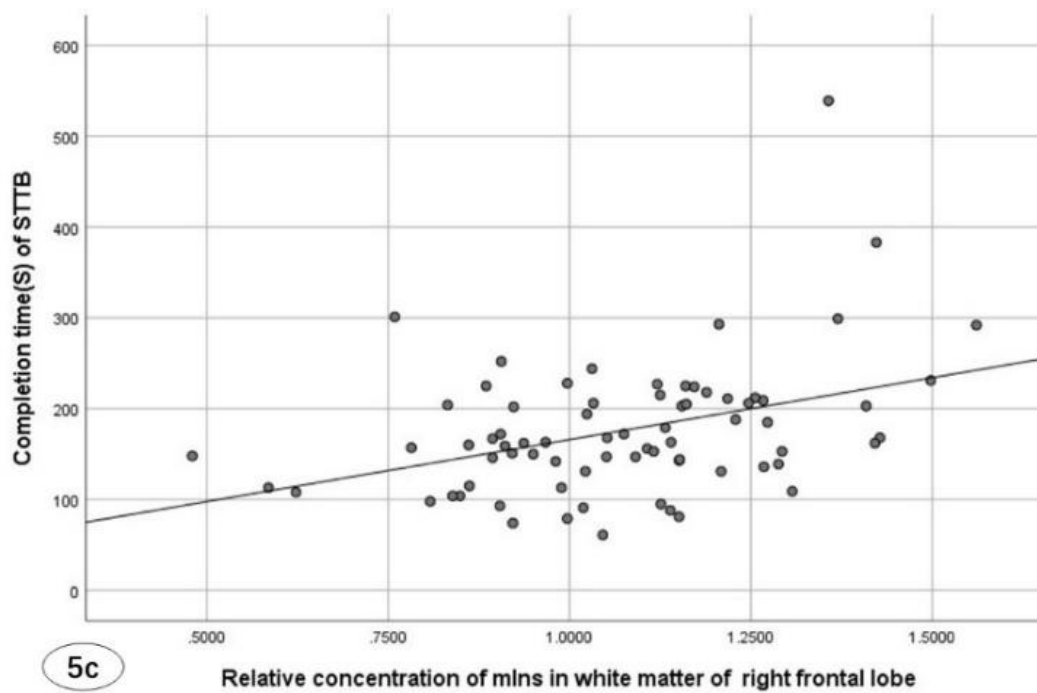
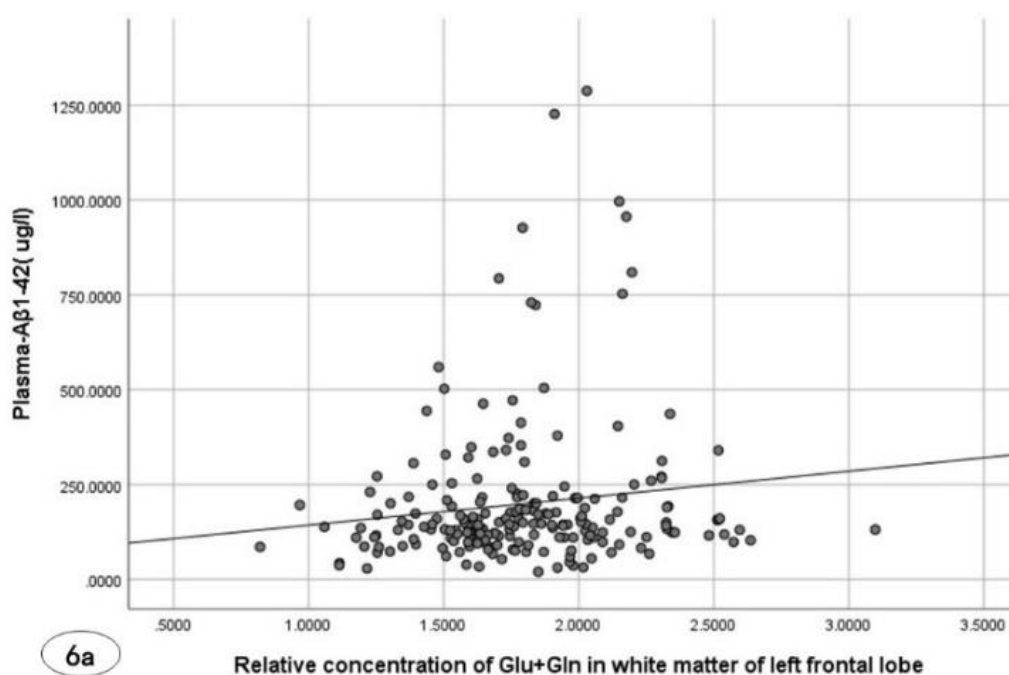


Figure 5. Associations between metabolite concentrations and neuropsychological test scores in the MCI group: (a) AVLT recognition and right frontal white matter NAA+NAAG; (b) STT-A completion time and right frontal white matter mIns; (c) STT-B completion time and right frontal white matter mIns.

In the MCI cohort, the AVLT recognition score exhibited a significant negative correlation with NAA+NAAG levels in the right frontal white matter ($r = -0.368$, $P = 0.001$; [Figure 5a](#)). Conversely, both STT-A ($r = 0.375$, $P < 0.001$; [Figure 5b](#)) and

STT-B ($r = 0.353$, $P = 0.002$; [Figure 5c](#)) completion times were positively associated with mIns concentrations in the same region. 3.3.

3.5. Association Between AD-related Genes, Blood Biomarkers, and Frontal White Matter Metabolites



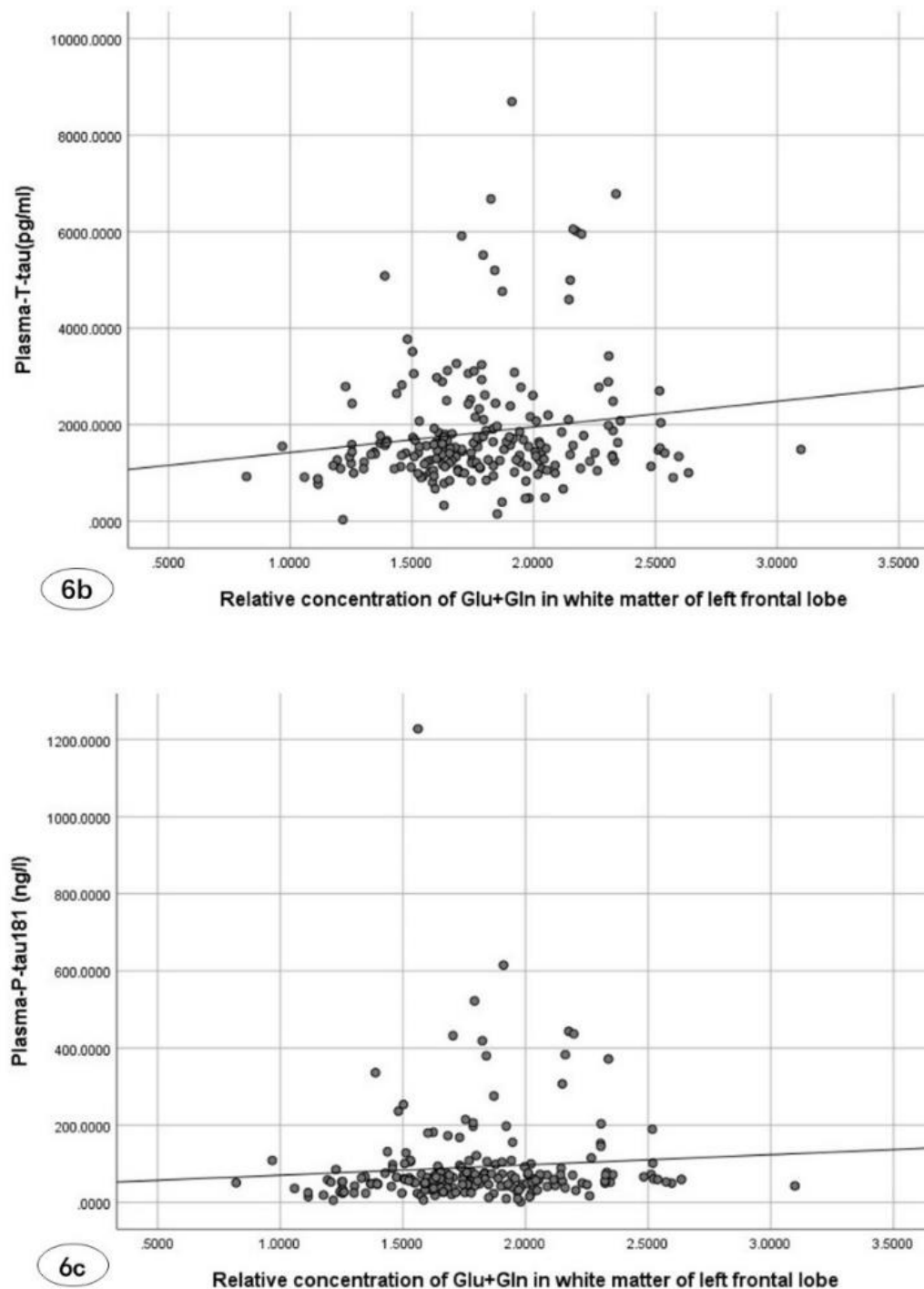


Figure 6. Associations between left frontal white matter Glu+Gln concentrations and (a) $A\beta 1-42$, (b) t -tau, and (c) p -tau181 levels.

ApoE- $\epsilon 4$ allele status was determined for 283 participants. No significant differences were observed in cognitive function, age, sex, or educational attainment between ApoE- $\epsilon 4$ carriers and non-carriers ($P > 0.05$). Similarly, relative metabolite concentrations in the bilateral frontal white matter did not differ significantly by ApoE- $\epsilon 4$ status (Mann-Whitney U test, $P > 0.05$). Detailed results are presented in Table 7.

Plasma levels of $A\beta 1-42$, t -tau, and p -tau181 were measured in 214 participants. No significant differences in these biomarkers were observed across cognitive groups (Kruskal-

Wallis test, all $P > 0.05$). However, the relative concentration of Glu+Gln in the left frontal white matter showed significant positive correlations with $A\beta 1-42$ ($r = 0.136$, $P = 0.049$; Figure 6a), t -tau ($r = 0.148$, $P = 0.032$; Figure 6b), and p -tau181 ($r = 0.169$, $P = 0.014$; Figure 6c).

4. Discussion

Emerging evidence suggests that neurochemical alterations

precede overt cognitive decline in neurodegenerative diseases [4, 5]. This multimodal study investigated 362 participants across the cognitive continuum (NC, SCD, SCD-p, and MCI) using single-voxel 1H-MRS of bilateral frontal white matter, combined with plasma biomarkers (A β 1-42, t-tau, p-tau181) and ApoE- ϵ 4 genotyping. Key findings are as follows. (1) Stage-Specific Cognitive Profiles: MCI subjects demonstrated significant impairment across memory, executive function, and language domains ($P < 0.01$). No significant differences were observed between SCD, SCD-p, and NC groups, supporting the preclinical nature of SCD. (2) Metabolic Lateralization: Healthy controls exhibited left-greater-than-right asymmetry in NAA+NAAG (+15.3%) and GPC+PCh (+12.7%) concentrations ($P < 0.05$). (3) Age-Related Metabolic Trajectories: Progressive NAA+NAAG reduction in left frontal white matter (28.6% decrease young \rightarrow elderly, $P < 0.01$). Elderly subjects showed 18.2% lower Glu+Gln levels versus young adults ($P < 0.01$), suggesting excitatory neurotransmission decline. (4) Biomarker Correlations: Right frontal NAA+NAAG negatively correlated with AVLT scores ($r = -0.368$). Right frontal mIns positively associated with STT completion times ($r = 0.35-0.38$). Left frontal Glu+Gln showed positive associations with plasma A β 1-42 ($r = 0.136$) and tau species ($r = 0.148-0.169$).

These findings highlight the potential of frontal lobe metabolomics for early detection of neurodegenerative processes.

4.1. In Vivo 1H-MRS Detection of Cerebral Metabolite Alterations in Cognitively Normal Participants

4.1.1. Impact of Hemispheric Asymmetry on Metabolite Concentrations in Bilateral Cerebral Hemispheres

The human brain consists of two cerebral hemispheres interconnected by the corpus callosum. These hemispheres exhibit distinct functional specialization, a phenomenon that progressively matures during ontogeny. In right-handed individuals, the left hemisphere is typically dominant [15]. Functionally, the left hemisphere governs language processing, logical reasoning, and numerical tasks, whereas the right hemisphere primarily mediates nonverbal functions such as visuospatial cognition and emotional regulation [16].

Neuroanatomical lateralization is also evident in the human brain. Right-handed individuals typically exhibit larger left frontal gray matter volume and an enlarged left transverse temporal gyrus, a key language-processing region, compared to the contralateral side [16]. PET imaging studies have demonstrated higher neuronal density, glucose metabolism, and cerebral blood flow in the left hemisphere relative to the right [17]. Using 1H-MRS on a 1.5T MR system, Cichocka et al. analyzed hemispheric metabolite differences in children aged 6–15 years. Sex-independent variations in NAA, Cr, Cho, mIns, LIPs, and LACs were observed in the hippocampus,

frontal lobe, and basal ganglia [18].

In this study, 1H-MRS using a 3.0T MR system was employed to assess the relative metabolite concentrations in the frontal white matter of right-handed, cognitively normal adults. The findings demonstrated that the left frontal white matter exhibited relatively higher levels of NAA+NAAG and GPC+PCho. NAA+NAAG alterations are associated with neuronal integrity, serving as indicators of neuronal activity and neurotransmitter levels [4, 5]. GPC+PCho, predominantly distributed in the cell membranes of neurons and glial cells, plays a central role in membrane synthesis and metabolism, functioning as a metabolic marker for cell proliferation and membrane integrity [4, 5]. These results suggest that, in right-handed cognitively normal subjects, the left frontal lobe displays greater neuronal activity, neurotransmitter levels, cell proliferation, and membrane integrity compared to the right frontal lobe, thereby reflecting the inherent asymmetry in neuronal distribution and function between the cerebral hemispheres in adults.

4.1.2. In Vivo 1H-MRS Detection of Metabolic Alterations in the Aging Brain

Recent in vivo 1H-MRS studies have yielded heterogeneous findings regarding neurochemical alterations associated with physiological brain aging [19-23]. The cerebral cortex remains the most frequently investigated region. A consensus has emerged that aging in adults is characterized by the following cortical metabolic changes [19-22]. NAA Reduction was observed in the lateral temporal lobe (TLAT), occipital cortex (OC), posterior cingulate gyrus (CING), medial temporal lobe (TMED), hippocampus (HIP), thalamus (THAL), insular cortex (INS), and cerebellar posterior lobe (CPOST). tCho elevation was detected in the THAL, splenium of the corpus callosum (SCC), and hand motor cortex (HCA). tCr increase was noted in the OC, HIP, and SCC.

This study demonstrated a significant age-dependent decline in the relative concentration of NAA+NAAG in the left frontal white matter. We hypothesize that this reduction may reflect diminished neuronal volume or density, as well as altered neurotransmitter levels in this region during aging. These neurochemical changes could underlie the physiological decline in cognitive functions associated with the left frontal lobe, such as memory formation and abstract reasoning [9].

This study also revealed an age-related trend toward decreased relative concentrations of Glu+Gln in the left frontal white matter, with the elderly group exhibiting significantly lower levels compared to both middle-aged and young groups. Previous research has suggested that age-dependent reductions in cerebral Glu levels are linked to cognitive and behavioral deficits, including impairments in learning and memory [23]. The observed decline in Glu+Gln concentrations in the elderly participants may reflect intrinsic brain aging processes and the associated neurochemical underpinnings of age-related cognitive deterioration.

4.2. Neurochemical Alterations in the Preclinical and Prodromal Phases of AD

The protracted trajectory of cognitive decline preceding AD dementia underscores the critical importance of early detection. In vivo 1H-MRS enables the monitoring of brain metabolite changes, thereby facilitating the identification of cognitive-related neuropathology during the preclinical stage, prior to the onset of irreversible neuronal damage [4, 5].

Research utilizing 1H-MRS to detect brain metabolites has predominantly focused on patients with AD dementia. A lower NAA/Cr ratio has been associated with synaptic integrity loss [24]. Notably, reduced NAA levels in AD dementia patients represent one of the most consistent findings compared to cognitively unimpaired (CU) individuals [4, 5, 25]. mIns, regarded as a glial marker and/or permeability regulator [26], serves as an indicator of neuroinflammation or inflammatory cell density [27]. Multiple studies have demonstrated elevated mIns or mIns/Cr ratios in various gray and white matter regions of AD dementia patients relative to controls [5, 25, 26]. Earlier investigations also reported diminished Glx levels in both AD dementia and MCI patients compared to CU participants [28, 29].

Two 1H-MRS studies focusing on the frontal cortex demonstrated that elevated plasma neurofilament light (NfL) levels were correlated with reduced tNAA/tCr and Glu/tCr ratios in the right dorsolateral prefrontal cortex of AD dementia patients [8]. Compared to CU participants, MCI patients exhibited higher GLX and mIns/tCr levels, along with lower GABA concentrations in the medial frontal cortex. Notably, GABA levels declined with age in both CU and MCI groups, yet no significant associations were observed between CSF biomarkers (β -amyloid 42, t-tau, and p-tau) and GABA or GABA/Cr ratios [10].

This study conducted a comparative analysis of NC, SCD, SCD-p, and MCI subjects, with covariance adjustment for age and educational attainment as confounding variables. The findings demonstrated no significant intergroup differences in bilateral frontal white matter metabolite concentrations across cognitive subgroups. However, within the MCI cohort, a negative correlation emerged between AVLT recognition scores and right frontal white matter NAA+NAAG levels. The AVLT recognition test serves as a sensitive measure of short-term memory capacity and represents a validated clinical tool for distinguishing cognitive impairment attributable to physiological aging, MCI, and AD [30].

While prior research has established an association between left temporal lobe NAA reduction and memory dysfunction [4, 5], our study identified an inverse relationship between right frontal white matter NAA+NAAG levels and short-term memory performance. This paradoxical finding suggests potential compensatory mechanisms involving frontal neuronal activity in MCI patients. We hypothesize that declining short-term memory may trigger a neurochemical compensatory response, manifested by elevated NAA/NAAG concentrations -

biomarkers of neuronal metabolic activity - to preserve central nervous system functionality.

This study further demonstrated a positive correlation between the relative concentration of mIns in the right frontal white matter and the completion times of both STT-A and STT-B tests in the MCI group. Specifically, higher mIns levels were associated with poorer executive function. Given that mIns alterations in brain parenchyma are indicative of reactive gliosis and localized neuroinflammatory responses following microstructural damage [19, 27], our findings suggest that elevated mIns in the right frontal cortex may serve as an indirect biomarker of executive dysfunction.

Certain metabolites identified via 1H-MRS exhibit associations with biological fluid biomarkers in AD [31-33]. Specifically, a reduced NAA/Cr ratio in the hippocampus (HIP) and cingulate cortex (CING) correlated with diminished CSF A β 42 levels, independent of CSF tau or pTau181 concentrations [31]. Longitudinal studies revealed a progressive decline in NAA/mIns ratios among CSF- β -positive individuals, particularly in the CING region [32]. Additionally, elevated Cho/Cr ratios were observed in CSF- β -positive MCI patients [33]. These findings underscore the heterogeneity and complexity of neurochemical alterations in the AD brain.

This study established a significant positive correlation between Glu+Gln concentrations in the left frontal white matter and cerebrospinal fluid biomarkers (A β 1-42, t-tau, p-tau181). Glutamate, as the central excitatory neurotransmitter, orchestrates critical neurophysiological processes including synaptic plasticity, memory formation, and excitotoxic cascades through its actions on ionotropic and metabotropic receptors [4, 5, 34]. Within the glutamate-glutamine cycle, glutamate serves as the metabolic precursor for GABA synthesis - the primary inhibitory neurotransmitter in the CNS [4, 5].

Notably, Riese et al. documented significant GABA depletion in amnesic MCI patients relative to age-matched controls [29]. Our findings suggest a potential pathophysiological cascade: elevated A β 1-42 deposition may induce neuronal dysfunction, disrupting local glutamate homeostasis. This metabolic disturbance manifests initially as impaired GABAergic transmission, subsequently triggering compensatory upregulation of glutamate-glutamine cycle activity to maintain excitatory-inhibitory balance in vulnerable neural circuits [4, 5].

Sun et al. demonstrated that exposure of hippocampal slices and primary neurons to glutamate induced hyperphosphorylation of tau protein at multiple AD-related epitopes [35]. In our study, the observed positive correlation between Glu+Gln concentrations and T-tau/P-tau181 levels further supports a potential regulatory interplay between glutamate-glutamine metabolism in the left frontal white matter and tau pathology. These findings suggest that 1H-MRS-detected alterations in Glu+Gln may serve as an indirect biomarker of in vivo tau and p-tau dynamics, offering clinicians novel insights into AD-related pathological mechanisms.

4.3. Limitation

This study has several noteworthy limitations. Firstly, while employing a prospective cohort design, the elderly NC subgroup was underpowered, necessitating future studies with larger geriatric cohorts to validate current findings. Secondly, the exclusive use of single-voxel PRESS sequences restricted metabolite assessment to bilateral frontal white matter, precluding comprehensive evaluation of whole-brain metabolic dynamics during cognitive progression. Thirdly, though our MCI cohort demonstrated correlations between NAA+NAAG/mIns levels and neuropsychological test performance (executive function/memory), longitudinal studies with standardized follow-up protocols are required to determine their clinical utility as cognitive monitoring biomarkers. Fourthly, the limited blood sample size constrains the generalizability of plasma biomarker findings, warranting expanded recruitment for robust validation. Lastly, the absence of consensus thresholds for plasma $\beta 1-42$, tau, and p-tau levels highlights the need for multimodal integration with advanced neuroimaging (Ultra-high field [$>3T$] MRI, PET-CT) and next-generation MRS techniques (sLASER) through multicenter longitudinal studies to elucidate biomarker synergies in AD pathogenesis.

5. Conclusions

The alterations in white matter metabolites within the bilateral frontal lobes, as detected by 1H-MRS, may serve as indicators of both physiological brain aging and potential associations with AD pathology. This study contributes foundational neurobiochemical data, offering an objective framework for elucidating cerebral laterality, age-related metabolic changes, and the early diagnostic potential of AD.

Abbreviations

AD	Alzheimer's Disease
A β	Amyloid β -protein
ANOVA	Analysis of Variance
AFT	Animal Fluency Test
AVLT-H	Auditory Verbal Learning Test
ApoE- ϵ 4	Apolipoprotein E- ϵ 4
BNT	Boston Naming Test
CU	Cognitively Unimpaired
EHI	Edinburgh Handedness Inventory
FAQ	Functional Activities Questionnaire
GABA	γ -aminobutyric Acid
GDS	Geriatric Depression Scale
GLX	Glutamate Complex
Glu	Glutamate
Glu+Gln	Glutamate and Glutamine
GPC	Glycerol-phosphocholine
HAMD	Hamilton Depression Scale

HAMA	Hamilton Anxiety Scale
MCI	Mild Cognitive Impairment
mIns	Myo-inositol
NAA	N-acetylaspartate
NAAG	N-acetyl Aspartyl-glutamate
NC	Normal Control
PCr	Phosphocreatine
PCho	Phosphocholine
PRESS	Point Resolved Spectroscopy
p-tau181	Phosphorylated Tau181
SCD	Subjective Cognitive Decline
SCD-p	SCD-plus
STT	Shape Trail Test
tCR	Total Creatine
t-tau	Total Tau

Acknowledgments

All authors would like to acknowledge Kang Sheng Da Medical Laboratory Co., Ltd. in Wuhan, Hubei Province for the detection of blood samples of this study. And to Gui-qing Wang (Statistician, Medical Record Management Department in Guangzhou First People's Hospital, School of Medicine, SCUT.) for her assistance in statistical analysis. And to all subjects, participants, medical personnel of Guangzhou First People's Hospital for their invaluable support. As well as Tencent Yuanbao for English language editing of this manuscript.

Author Contributions

Qi Xie: Conceptualization, Data curation, Funding acquisition, Project administration, Writing – original draft, Writing – review & editing

Zhi-lin Tan: Data curation, Formal Analysis, Investigation, Writing – original draft

Ya-jie Wang: Investigation, Methodology, Writing – original draft

Hui-xian Chen: Data curation, Investigation, Methodology, Writing – original draft

Funding

This work is supported by funding from the Guangzhou Science and Technology Plan Project (No. 201907010020) as well as the People's Livelihood Science and Technology Project in Nansha District, Guangzhou (No. 2021MS007), and Guangzhou Health Science and Technology Project (No. 20251A010002).

Data Availability Statement

The data is available from the corresponding author upon reasonable request.

Conflicts of Interest

The authors declare no conflicts of interest.

Appendix

Tables 1-7

Table 1. Basic information and scale scores of different cognitive groups ($\bar{X}\pm S$).

Index	NC group (n=108)	SCD group (n=97)	SCD-Plus group (n=79)	MCI group (n=78)	P value
Age (year)	40.62±13.09	47.09±13.53 ^a	46.13±13.87	55.36±10.94 ^{abc}	<0.001
Male/Female	65/43	44/53	33/46	36/42	0.050
Education duration	14.99±3.34	13.56±3.54 ^a	14.23±3.74	10.80±2.83 ^{abc}	<0.001
Memory (Z value)	0.79±1.33	0.56±1.50	0.23±1.56	-2.03±1.43 ^{abc}	<0.001
AVLT-N5	6.59±2.16	6.16±2.48	5.73±2.67	2.95±1.89 ^{abc}	<0.001
AVLT-N7	22.20±1.55	22.07±1.72	21.66±1.78	18.99±2.24 ^{abc}	<0.001
Execution (Z value)	0.31±1.56	0.30±2.14	0.13±1.68	-0.93±1.33 ^{abc}	<0.001
STT-A (s)	40.80±12.90	47.36±15.52 ^a	46.46±13.80	66.32±29.11 ^{abc}	<0.001
STT-B (s)	109.05±43.67	123.36±55.41	119.19±45.42	175.93±73.78 ^{abc}	<0.001
Language (Z value)	0.57±1.38	0.34±1.52	0.40±1.46	-1.62±1.69 ^{abc}	<0.001
AFT	19.43±4.15	18.74±4.78	18.99±4.08	14.88±4.20 ^{abc}	<0.001
BNT	23.19±3.19	22.82±3.38	22.87±3.36	18.18±4.16 ^{abc}	<0.001

Note: P-value <0.05 denotes statistical significance. Superscript 'a' indicates significant differences in post hoc comparisons with the NC group; 'b' denotes significant differences versus the SCD group; and 'c' signifies significant differences relative to the SCD-Plus group. Higher Z-scores reflect superior cognitive performance.

Table 2. Comparison of relative concentrations of metabolites in bilateral frontal white matter ($\bar{X}\pm S$).

Metabolite	Left	Right	P value
NAA+NAAG	1.54±0.20	1.38±0.18	<0.001*
GPC+PCh	0.42±0.06	0.40±0.05	0.008*
mIns	0.99±0.21	1.06±0.22	0.052
Glu+Gln	1.81±0.39	1.73±0.38	0.159

Note: *P<0.05 indicates the statistically significant difference, Mann Whitney U test.

Table 3. Comparison of relative concentrations of metabolites among different ages ($\bar{X}\pm S$).

Index	Youth group (n=65)	Middle-aged group (n=30)	Older group (n=13)	P value
Gender (Male/Female)	36/29	19/11	10/3	0.322

Index		Youth group (n=65)	Middle-aged group (n=30)	Older group (n=13)	P value
Education duration (year)		16.28±2.47	13.95±3.49 ^a	10.92±2.81 ^{ab}	<0.001*
NAA+NAAG	L	1.60±0.19	1.46±0.18 ^a	1.39±0.20 ^{ab}	<0.001*
	R	1.37±0.18	1.38±0.18	1.44±0.20	0.741
GPC+PCh	L	0.42±0.06	0.41±0.05	0.42±0.05	0.359
	R	0.39±0.06	0.41±0.04	0.42±0.05	0.087
mIns	L	0.94±0.21	1.07±0.17	1.09±0.23	0.078
	R	1.08±0.23	1.01±0.17	1.05±0.28	0.152
Glu+Gln	L	1.86±0.37	1.83±0.42	1.52±0.25 ^{ab}	0.008*
	R	1.73±0.37	1.78±0.45	1.63±0.27	0.373

Note: *P-value <0.05 denotes statistical significance. Superscript 'a' indicates significant differences compared to the young group, and 'b' denotes significant differences versus the middle-aged group. L: Left; R: Right.

Table 4. Comparison of relative concentrations of metabolites between different genders.

Metabolite		Male (n=65)	Female (n=43)	P value
Age (year)		42.66±12.68	36.54±11.93	0.046*
Education duration (year)		14.45±3.52	15.79±2.96	0.080
NAA+NAAG	Left	1.51±0.20	1.58±0.20	0.440
	Right	1.38±0.17	1.39±0.20	0.595
GPC+PCh	Left	0.42±0.05	0.42±0.06	0.896
	Right	0.40±0.05	0.39±0.05	0.843
mIns	Left	1.03±0.20	0.95±0.22	0.171
	Right	1.04±0.23	1.08±0.20	0.539
Glu+Gln	Left	1.85±0.36	1.75±0.43	0.068
	Right	1.75±0.44	1.71±0.29	0.479

Note: *P<0.05 indicates the statistically significant difference, Mann Whitney U test.

Table 5. Demographic characteristics across age subgroups.

Group		Gender (Male/Female)	Age (year)	Education duration (year)
Youth group	NC (n=65)	36/29	31.68±6.60	16.28±2.47
	SCD (n=46)	17/29	35.30±5.80	15.35±3.11
	SCD-P (n=41)	19/22	34.56±5.64	15.13±3.40
	MCI (n=14)	9/5	37.36±6.45	12.79±2.23
	P value	0.161	0.002*	<0.001*
Middle-aged group	NC (n=30)	19/11	49.93±4.32	13.95±3.49
	SCD (n=30)	19/11	51.30±3.98	12.77±2.98

Group		Gender (Male/Female)	Age (year)	Education duration (year)
Older group	SCD-P (n=21)	11/10	52.86±4.16	14.48±4.02
	MCI (n=34)	12/22	53.71±3.60	10.40±3.10
	<i>P</i> value	0.052	0.002*	<0.001*
	NC (n=13)	10/3	63.85±4.06	10.92±2.81
	SCD (n=21)	8/13	66.90±4.64	10.76±3.01
	SCD-P (n=17)	3/14	65.71±5.19	11.76±3.23
	MCI (n=30)	15/15	65.63±3.94	10.33±2.41
	<i>P</i> value	0.011*	0.194	0.559

Note: * $P < 0.05$ indicates the statistically significant difference. χ^2 test was used for gender, and K-W test was used for age and education duration.

Table 6. Relative metabolite concentrations in bilateral frontal white matter stratified by age across cognitive diagnostic groups.

Group		NAA+NAAG		GPC+PCh		mIns		Glu+Gln	
		Left	Right	Left	Right	Left	Right	Left	Right
Youth group	NC (n=65)	1.60±0.19	1.37±0.18	0.42±0.06	0.39±0.06	0.94±0.21	1.08±0.23	1.86±0.36	1.73±0.38
	SCD (n=46)	1.60±0.16	1.39±0.16	0.42±0.06	0.39±0.06	0.95±0.18	0.96±0.17	1.87±0.28	1.77±0.35
	SCD-P (n=41)	1.57±0.18	1.39±0.26	0.41±0.05	0.42±0.11	0.99±0.21	1.04±0.22	1.89±0.38	1.65±0.31
	MCI (n=14)	1.56±0.19	1.37±0.17	0.41±0.05	0.41±0.07	0.98±0.24	1.06±0.18	1.85±0.30	1.71±0.30
	<i>P</i> value	0.802	0.948	0.411	0.360	0.735	0.119	0.953	0.443
Middle-aged group	NC (n=26)	1.46±0.18	1.38±0.18	0.41±0.05	0.41±0.04	1.07±0.17	1.01±0.17	1.83±0.40	1.78±0.42
	SCD (n=26)	1.46±0.18	1.43±0.18	0.41±0.06	0.42±0.04	1.04±0.18	0.99±0.20	1.69±0.24	1.79±0.53
	SCD-P (n=18)	1.44±0.19	1.41±0.17	0.45±0.06	0.41±0.05	1.06±0.18	1.03±0.15	1.58±0.29	1.75±0.39
	MCI (n=32)	1.49±0.15	1.39±0.16	0.41±0.05	0.42±0.05	1.07±0.22	0.99±0.19	1.71±0.35	1.85±0.49
	<i>P</i> value	0.488	0.603	0.113	0.436	0.838	0.368	0.148	0.912
Older group	NC (n=13)	1.39±0.20	1.44±0.20	0.42±0.05	0.42±0.05	1.09±0.23	1.05±0.28	1.52±0.42	1.63±0.25
	SCD (n=21)	1.41±0.16	1.40±0.12	0.43±0.05	0.41±0.06	1.06±0.15	1.17±0.15	1.70±0.33	1.87±0.36
	SCD-P (n=17)	1.40±0.15	1.44±0.21	0.41±0.05	0.42±0.07	1.03±0.15	1.10±0.20	1.65±0.32	1.86±0.32
	MCI (n=30)	1.43±0.22	1.43±0.21	0.42±0.06	0.44±0.04	1.08±0.19	1.17±0.21	1.77±0.39	1.93±0.43
	<i>P</i> value	0.827	0.900	0.603	0.170	0.712	0.268	0.113	0.262

Table 7. Relative metabolite concentrations in bilateral frontal white matter stratified by ApoE- ϵ 4 carrier status.

Item	ApoE- ϵ 4+(n=52)	ApoE- ϵ 4-(n=231)	<i>P</i> value
Gender (Male/Female)	25/27	113/118	0.586
Age (year)	48.92±12.63	46.44±13.56	0.239
Education duration (year)	12.81±3.68	13.65±3.88	0.272
NAA+NAAG Left	1.51±0.20	1.53±0.19	0.738

Item		ApoE-ε4+(n=52)	ApoE-ε4-(n=231)	P value
GPC+PCh	Right	1.40±0.16	1.38±0.19	0.959
	Left	0.43±0.05	0.42±0.05	0.389
	Right	0.42±0.05	0.41±0.07	0.214
mIns	Left	1.05±0.17	1.02±0.20	0.276
	Right	1.05±0.24	1.04±0.20	0.761
Glu+Gln	Left	1.82±0.43	1.78±0.34	0.646
	Right	1.75±0.32	1.77±0.40	0.762

Note: *P<0.05 indicates the statistically significant difference.

References

- [1] Villain N, Michalon R. What is Alzheimer's disease? An analysis of nosological perspectives from the 20th and 21st centuries. *Eur J Neurol* 2024; 31(11): e16302. <https://doi.org/10.1111/ene.16302>
- [2] D'elia Y, Whitfield T, Schlosser M, et al. Impact of mindfulness-based and health self-management interventions on mindfulness, self-compassion, and physical activity in older adults with subjective cognitive decline: A secondary analysis of the SCD-Well randomized controlled trial. *Alzheimers Dement (Amst)* 2024; 16(1): e12558. <https://doi.org/10.1002/dad2.12558>
- [3] Botello-Marabotto M, Martínez-Bisbal MC, Calero M, et al. Non-invasive biomarkers for mild cognitive impairment and Alzheimer's disease. *Neurobiol Dis* 2023; 187: 106312. <https://doi.org/10.1016/j.nbd.2023.106312>
- [4] Kara F, Kantarci K. Understanding Proton Magnetic Resonance Spectroscopy Neurochemical Changes Using Alzheimer's Disease Biofluid, PET, Postmortem Pathology Biomarkers, and APOE Genotype. *Int J Mol Sci* 2024; 25(18): 10064. <https://doi.org/10.3390/ijms251810064>
- [5] McKiernan E, Su L, O'Brien J. MRS in neurodegenerative dementias, prodromal syndromes and at-risk states: A systematic review of the literature. *NMR Biomed* 2023; 36(7): e4896. <https://doi.org/10.1002/nbm.4896>
- [6] Dubois B, Villain N, Frisoni GB, et al. Clinical diagnosis of Alzheimer's disease: recommendations of the International Working Group. *Lancet Neurol* 2021; 20(6): 484-496. [https://doi.org/10.1016/S1474-4422\(21\)00066-1](https://doi.org/10.1016/S1474-4422(21)00066-1)
- [7] Palmqvist S, Schöll M, Strandberg O, et al. Earliest accumulation of β-amyloid occurs within the default-mode network and concurrently affects brain connectivity. *Nat Commun* 2017; 8(1): 1214. <https://doi.org/10.1038/s41467-017-01150-x>
- [8] Matsuoka K, Hirata K, Kokubo N, et al. Investigating neural dysfunction with abnormal protein deposition in Alzheimer's disease through magnetic resonance spectroscopic imaging, plasma biomarkers, and positron emission tomography. *Neuroimage Clin* 2024; 41: 103560. <https://doi.org/10.1016/j.nicl.2023.103560>
- [9] Tullberg M, Fletcher E, DeCarli C, et al. White matter lesions impair frontal lobe function regardless of their location. *Neurology* 2004; 63(2): 246-53. <https://doi.org/10.1212/01.wnl.0000130530.55104.b5>
- [10] Hone-Blanchet A, Bohsali A, Krishnamurthy LC, et al. Frontal Metabolites and Alzheimer's Disease Biomarkers in Healthy Older Women and Women Diagnosed with Mild Cognitive Impairment. *J Alzheimers Dis* 2022; 87(3): 1131-1141. <https://doi.org/10.3233/JAD-215431>
- [11] Chen H-X. Functional magnetic resonance imaging-based exploration of mild cognitive impairment and the relationship between visual response and cognition [D]. Guangzhou Medical University, 2019.
- [12] Tang Z-L. In vivo detection of metabolites in bilateral frontal white matter and their correlation with cognitive function based on proton magnetic resonance spectroscopy [D], South China University of Technology, Guangzhou, 2021.
- [13] Ahmad, O, Boschipinto C, Lopez A, et al. (2002). Age standardization of rates: a new WHO standard (GPE discussion paper Series: No. 31).
- [14] Xie Q, Xu H-X, Wang Y-J, et al. In vivo quantification of superficial cortical veins on susceptibility-weighted imaging with artificial intelligence image segmentation and the potential mechanism of human cognitive decline. *Front. Aging Neurosci.* 2025; 17: 1557397. <https://doi.org/10.3389/fnagi.2025.1557397>
- [15] Dexheimer B, Sainburg R, Sharp S, et al. Roles of Handedness and Hemispheric Lateralization: Implications for Rehabilitation of the Central and Peripheral Nervous Systems: A Rapid Review. *Am J Occup Ther* 2024; 78(2): 7802180120. <https://doi.org/10.5014/ajot.2024.050398>
- [16] Wan B, Saberi A, Paquola C, et al. Microstructural asymmetry in the human cortex. *Nat Commun.* 2024 Nov 22; 15(1): 10124. <https://doi.org/10.1038/s41467-024-54243-9>

- [17] Jayasundar R. Human brain: biochemical lateralization in normal subjects. *Neurol India* 2002; 50(3): 267-71. <https://doi.org/10.1007/s100720200100>
- [18] Cichocka M, Kozub J, Karcz P, et al. Differences in Metabolite Concentrations Between the Hemispheres of the Brain in Healthy Children: A Proton Magnetic Resonance Spectroscopy Study (1HMRS). *J Child Neurol* 2016; 31(11): 1296-301. <https://doi.org/10.1177/0883073816653784>
- [19] Mahmoudi N, Dadak M, Bronzlik P, et al. Microstructural and Metabolic Changes in Normal Aging Human Brain Studied with Combined Whole-Brain MR Spectroscopic Imaging and Quantitative MR Imaging. *Clin Neuroradiol* 2023; 33(4): 993-1005. <https://doi.org/10.1007/s00062-023-01300-3>
- [20] Maghsudi H, Schütze M, Maudsley AA, et al. Age-related Brain Metabolic Changes up to Seventh Decade in Healthy Humans: Whole-brain Magnetic Resonance Spectroscopic Imaging Study. *Clin Neuroradiol* 2020; 30(3): 581-589. <https://doi.org/10.1007/s00062-019-00814-z>
- [21] Eylers VV, Maudsley AA, Bronzlik P, et al. Detection of Normal Aging Effects on Human Brain Metabolite Concentrations and Microstructure with Whole-Brain MR Spectroscopic Imaging and Quantitative MR Imaging. *Am J Neuroradiol* 2016; 37(3): 447-54. <https://doi.org/10.3174/ajnr.A4557>
- [22] Maghsudi H, Schmitz B, Maudsley AA, et al. Regional Metabolite Concentrations in Aging Human Brain: Comparison of Short-TE Whole Brain MR Spectroscopic Imaging and Single Voxel Spectroscopy at 3T. *Clin Neuroradiol* 2020; 30(2): 251-261. <https://doi.org/10.1007/s00062-018-00757-x>
- [23] Thomson AR, Hwa H, Pasanta D, et al. The developmental trajectory of 1H-MRS brain metabolites from childhood to adulthood. *Cereb Cortex* 2024; 34(3): bhae046. <https://doi.org/10.1093/cercor/bhae046>
- [24] Murray ME, Przybelski SA, Lesnick TG, et al. Early Alzheimer's disease neuropathology detected by proton MR spectroscopy. *J Neurosci* 2014; 34(49): 16247-55. <https://doi.org/10.1523/JNEUROSCI>
- [25] Kantarci K, Jack CR Jr, Xu YC, et al. Regional metabolic patterns in mild cognitive impairment and Alzheimer's disease: A 1H MRS study. *Neurology* 2000; 55(2): 210-7. <https://doi.org/10.1212/wnl.55.2.210>
- [26] Rae CD. A guide to the metabolic pathways and function of metabolites observed in human brain 1H magnetic resonance spectra. *Neurochem Res* 2014; 39(1): 1-36. <https://doi.org/10.1007/s11064-013-1199-5>
- [27] Nutma E, Fancy N, Weinert M, et al. Translocator protein is a marker of activated microglia in rodent models but not human neurodegenerative diseases. *Nat Commun* 2023; 14(1): 5247. <https://doi.org/10.1038/s41467-023-40937-z>
- [28] Zeydan B, Deelchand DK, Tosakulwong N, et al. Decreased Glutamate Levels in Patients with Amnesic Mild Cognitive Impairment: An sLASER Proton MR Spectroscopy and PiB-PET Study. *J Neuroimaging* 2017; 27(6): 630-636. <https://doi.org/10.1111/jon.12454>
- [29] Riese F, Gietl A, Zölch N, et al. Posterior cingulate γ -aminobutyric acid and glutamate/glutamine are reduced in amnesic mild cognitive impairment and are unrelated to amyloid deposition and apolipoprotein E genotype. *Neurobiol Aging* 2015; 36(1): 53-9. <https://doi.org/10.1016/j.neurobiolaging.2014.07.030>
- [30] Estevez-Gonzalez A, Kulisevsky J, Boltes A, et al. Rey verbal learning test is a useful tool for differential diagnosis in the pre-clinical phase of Alzheimer's disease: comparison with mild cognitive impairment and normal aging. *Int J Geriatr Psychiatry*, 2003; 18(11): 1021-1028. <https://doi.org/10.1002/gps.1010>
- [31] Bittner DM, Heinze HJ, Kaufmann J. Association of 1H-MR spectroscopy and cerebrospinal fluid biomarkers in Alzheimer's disease: diverging behavior at three different brain regions. *J Alzheimers Dis* 2013; 36(1): 155-63. <https://doi.org/10.3233/JAD-120778>
- [32] Waragai M, Moriya M, Nojo T. Decreased N-Acetyl Aspartate/Myo-Inositol Ratio in the Posterior Cingulate Cortex Shown by Magnetic Resonance Spectroscopy May Be One of the Risk Markers of Preclinical Alzheimer's Disease: A 7-Year Follow-Up Study. *J Alzheimers Dis* 2017; 60(4): 1411-1427. <https://doi.org/10.3233/JAD-170450>
- [33] Voevodskaya O, Sundgren PC, Strandberg O, et al. Myo-inositol changes precede amyloid pathology and relate to APOE genotype in Alzheimer disease. *Neurology* 2016; 86(19): 1754-61. <https://doi.org/10.1212/WNL.0000000000002672>
- [34] Geerts H. Indicators of neuroprotection with galantamine. *Brain Res Bull* 2005; 64(6): 519-24. <https://doi.org/10.1016/j.brainresbull.2004.11.002>
- [35] Sun XY, Wei YP, Xiong Y, et al. Synaptic released zinc promotes tau hyperphosphorylation by inhibition of protein phosphatase 2A (PP2A). *J Biol Chem* 2012; 287(14): 11174-82. <https://doi.org/10.1074/jbc.M111.309070>